EUROPEAN JOURNAL OFMATERIALS SCIENCE AND ENGINEERING
Volume 2, Issue 2-3, 2017: 77-82|www.ejmse.tuiasi.ro| ISSN: 2537-4338

EFFECT OF N ION IMPLANTATION ON STRUCTURAL, MORPHOLOGICAL AND MAGNETIC PROPERTIES OF CeO_2 THIN FILMS ON Al_2O_3 SUBSTRATES

Pawan KUMAR[1*], Zubida HABIB[2],

[1]Department of Physics, Kurukshetra University Kurukshetra, Haryana – 136119, India
[2]Department of Chemistry, National Institute of Technology, Hazratbal, Srinagar – 190006, India

Abstract

The present study reports the structural, morphological and magnetic properties of 80 keV N ion implanted CeO_2 thin films deposited over Al_2O_3 substrates by RF sputtering technique. The implantation was carried out at the fluence of 1×10^{16} ions/cm^2, 3×10^{16} ions/cm^2 and 6×10^{16} ions per cm^2, respectively. X-ray diffraction analysis confirmed the formation of face-centered cubic (FCC) structure corresponds to CeO_2. The surface morphology images indicate the increase in surface roughness value of the thin films after N ion implantation. The saturation magnetization in pristine thin film is found more as compared to N ion implanted films. It is observed that the saturation magnetization suppresses after N ion implantation. F-center exchange mechanism which is based on defects such as oxygen vacancies play significant role behind such ferromagnetic behavior.

Keywords:CeO_2*, Ion implantation, Magnetic properties*

Introduction

Rare earth materials have received significant attention due to their potential and technological applications such as biosensors, catalytic converters, lithium ion batteries and magnets. CeO_2 is one of the most important rare earth metal oxides and has been extensively studied for several technological applications [1-5]. The physical properties of CeO_2 can be greatly influenced by particle size, doping and synthesis methods [6]. Doped CeO_2 nanoparticles are promising electrolyte materials for SOFC [7]. The capacity of the modern automotive exhaust treatment catalysts containing CeO_2 is much more effective than that of the predecessors due to its high ''oxygen storage capacity''. Most recently, CeO_2 nanoparticles have been tested for their ability to serve as free-radical scavengers [8-9] to provide protection against chemical, biological, and radiological insults that promote the production of free radicals. Therefore, the extensive synthesis of CeO_2 becomes an urgent task for further research and applications [10-11]. Recently, finding of room temperature ferromagnetism in CeO_2 has been a subject of research due to the importance in spintronics.

The material's modification with energetic ion beams has emerged with interesting technological aspects and has resulted in significant progress in miniaturization of devices. There are two modes of materials modification by energetic ion beams, ion implantation and swift heavy ion (SHI) irradiation. In both of the techniques, the energy and fluence of incident ions play an important role [12]. In the ion implantation process, the energetic ions have low

Corresponding author: pawansaroha500@gmail.com

energy (a few tens of keV to a few hundreds of keV). The desired ions can be implanted in the suitable material by choosing the various implantation parameters like type of ion, ion energy, range of ion and ion fluence etc. and the materials properties get modified due to the presence of implanted ions. There are several reports available on the formation of embedded nano phases of target ions and effects of such nano phases on the various properties of host material [13-14]. In this context we have performed ion implantation experiment with different fluencies on CeO_2 thin films.

Considering the importance of these materials, present study focuses on understanding of structural, morphological and magnetic properties of N ion implanted CeO_2 thin films deposited by RF sputtering.

Experimental details

CeO_2 thin films were deposited on Al_2O_3 substrates using RF sputtering. The deposition was carried out by keeping RF power of 150 W in the Ar gas environment at room temperature. The films were then implanted with 80 keV of N ion beam having current of 2 μA using low energy ion beam facility (LEIBF) at Inter University Accelerator Centre (IUAC), New Delhi. The implantation was performed at three fluences; 1×10^{16}, 3×10^{16} and 6×10^{16} ions per cm^2. The structural, morphological and magnetic properties of the pristine and N ion implanted films were then systematically investigated by using various techniques. X-ray diffraction (XRD) measurement was carried out using Bruker D8 x-ray diffractometer (CuKα radiation; λ=1.54 Å) to obtain structural information within 20–60^o range with a step size of 0.02^o. The surface morphology was examined by a Multi Mode Scanning Probe Microscopy with Nanoscope IIIa controller from Digital/Veeco Instruments Inc. in tapping mode using RTESP tip. The magnetic properties were investigated using vibrating sample magnetometer (VSM) (MicroSense EZ9 VSM).

Results and Discussion

Structural properties

Figure 1display the XRD pattern of pristine and N ion implanted CeO_2 thin films. This shows formation of the fluorite-like (FCC) structure in all films corresponds to CeO_2. It is observed that the N ion implantation results in the variation of peak intensity compared to pristine film (see figure 1). The average crystallite size was estimated using Scherrer's equation as shown below [15],

$$D=0.9\lambda/\beta cos\theta \tag{1}$$

Where 'D' is the crystallite size, 'λ' (1.54 Å) is the wavelength of the incident x-rays, 'β' is the full width at half maximum (FWHM) and 'θ' is the Bragg angle of reflection, respectively. The estimated values of crystallite size and FWHM values are given in table 1 and it is evident that crystallite size increases at higher N fluence (3×10^{16} ions/cm^2 and 6×10^{16} ions per/cm^2) and FWHM decreases at these same fluence as compared to pristine film.

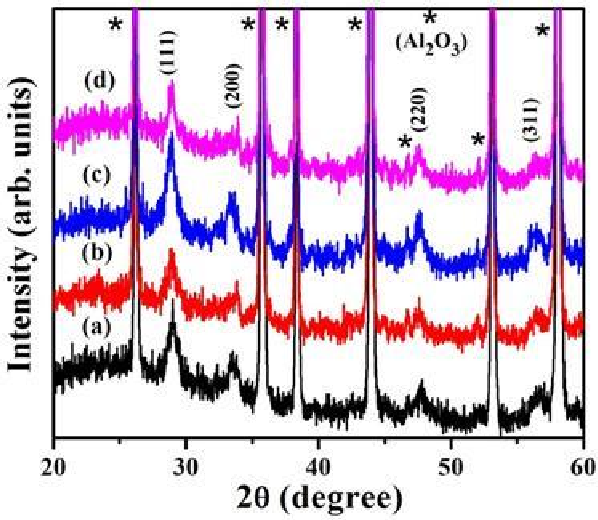

Fig.1. XRD pattern of (a) pristine, (b) $1x10^{16}$ ions/cm^2, (c) $3x10^{16}$ ions/cm^2 and (d) $6x10^{16}$ ions/cm^2 N ion implanted CeO_2 thin films

Surface morphological studies

Figure 2 shows the surface morphological images of pristine and N ion implanted CeO_2 thin films. The formation of circular-shape like grains in case of pristine film can be clearly seen. However, the surface morphology of the grains in N ion implanted is very different compared to pristine film. The smaller grains have been agglomerated on the surface in case of N ion implanted films. The calculated values for the average grain size and root mean square (RMS) surface roughness of the pristine, 1×10^{16} ions/cm^2 and 6×10^{16} ions/cm^2 N ion implanted films are listed in table 1. After the N ion implantation, the surface roughness and grain size values increases with increasing N ion fluence (table 1).

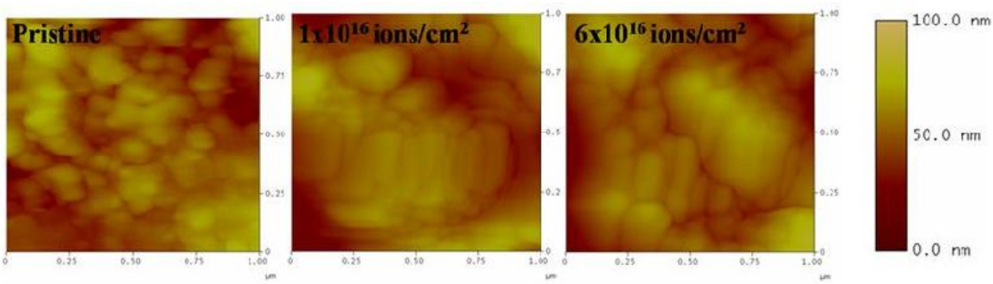

Fig.2. AFM images of pristine and N ion implanted CeO_2 thin films.

Magnetic measurements

Figure 3 presents the magnetization (M) versus applied field (H) plot of pristine and N ion implanted CeO_2 thin films at room temperature. It is clearly seen that all the films show ferromagnetic behavior. However the non-monotonic behavior of these films with applied field is due to diamagnetic contribution of Al_2O_3 substrates as shown in inset of Figure 3. The saturation magnetization (M_s) values of pristine and N ion implanted films are given in table 1. It is observed that the M_s is higher for pristine film as compared to N ion implanted films. The

M_s was found to be decreased after N ion implantation. It is possible that when N ion substitutes at a divalent oxygen ion there is a charge imbalance in the lattice as well as variation in the number of defects, i.e. oxygen vacancies, hence decrease the M_s in N ion implanted films.

The oxygen vacancy based F-center exchange mechanism is suitable to explain the ferromagnetic properties in oxides. There are three possible charge states of the existence of oxygen vacancy (V_O): (a) F^{2+} center, when no electron is trapped, (b) F^{+} center, when one electron is trapped in V_O which can mediate FM ordering (c) F^{0} center, when two electrons are trapped in V_O show singlet (S = 0) state which mediate weak antiferromagnetic ordering [16, 17]. In the present study, it might be possible that the with N ion implantation F^{2+} and F^{0} are more pronounced compared to F^{+} defects which result suppression of M_s in N implanted films compared to pristine film.

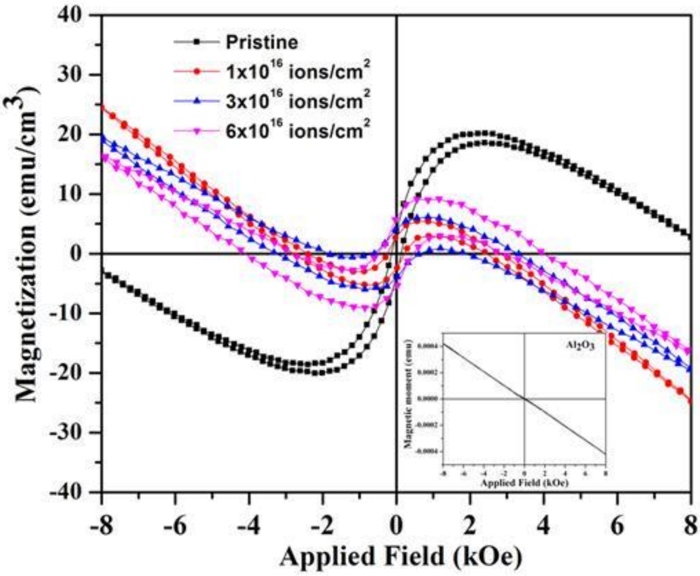

Fig.3. Room temperature M-H plot of Pristine and N ion implanted CeO_2 thin films.

Table 1 Various calculated parameters of pristine and N ion implanted films.

Sample	Crystallite size (nm)	FWHM	Grain size (nm)	Roughness (nm)	Saturation magnetization (M_s)
Pristine	10.08	0.8137	112.5	11.5	20.45
1x10^{16} ions/cm^2	9.36	0.8763	165.63	15.12	5.12
3x10^{16} ions/cm^2	10.47	0.7831	_	_	6.29
6x10^{16} ions/cm^2	16.57	0.4951	202.34	21.33	9.37

Conclusion

In this work, we investigated the structural, morphological and magnetic properties of pristine and N ion implanted CeO_2 thin films. The CeO_2 thin films were deposited on Al_2O_3 substrate using RF sputtering technique, and implanted with N ion at fluences of 1×10^{16}, 3×10^{16} and 6×10^{16} ions per cm^2 respectively. These films were characterized using XRD, AFM and magnetic measurements. The XRD result confirmed the formation of FCC structure in all CeO_2 films. The AFM images show large change in surface morphology of these films after N ion implantation. The magnetic measurement results showed suppression of saturation magnetization after N ion implantation. It is proposed that the distribution of N ions inside the host CeO_2 lattice creates various kinds of defects and play a significant role in the magnetic properties of these films.

Acknowledgments

One of the authors Pawan Kumar would like to acknowledge CSIR, New Delhi for providing the SRF-fellowship. The author is also very gratefully thankful to Department of Physics, Kashmir University for magnetic measurements and IUC-DAE, Indore for other experimental support.

References

[1] D. P. Norton, *Synthesis and Properties of Epitaxial Electronic Oxide Thin-Film Materials*, **Materials Science and Engineering, 43**, 2004, 139−247.

[2] M. Das, C. Dhand, G. Sumana, A. K. Srivastava, N. Vijayan, R. Nagarajan and B. D. Malhotra, *Zirconia grafted carbon nanotubes based biosensor for M. Tuberculosis detection*, **Applied Physics Letter**, **99**, 2011, 143702–143704.

[3] D. Patil, N. Q. Dung, H. Jung, S. Y. Ahn, D. M. Jang and D. Kim, *Enzymatic glucose biosensor based on CeO_2 nanorods synthesized by non-isothermal precipitation*, **Biosensors and Bioelectronics, 31**, 2012, 176–181.

[4] Y. Hinatsu and Y. Doi, *Magnetic properties and structural transitions of fluorite-related rare earth osmates Ln3OsO7 (Ln=Pr, Tb)*, **Journal of Solid State Chemistry, 198**, 2013, 176–185.

[5] G. Niu, E. Hildebrandt, M. A. Schubert, F. Boscherini, M. H. Zoellner, L. Alff, D. Walczyk, P. Zaumseil, I. Costina, H. Wilkens and T. Schroeder, *Oxygen Vacancy Induced Room Temperature Ferromagnetism in Pr Doped CeO_2 Thin Films on Silicon*, **ACS Applied Materials & Interfaces, 6**, 2014, 17496–17505

[6] M. Kamruddin, P. K. Ajikumar, R. Nithya, G. Mangamma, A. K. Tyagi and R. Baldev, *Effect of water of crystallization on synthesis of nanocrystalline ceria by non-hydrolytic method*, **Powder Technology, 161,** 2006, 145–149.

[7] C. Xia, Y. Cai, Y. Ma, B. Wang, W. Zhang, M. Karlsson,Y. W, and B. Zhu, *Natural Mineral-Based Solid Oxide Fuel Cell with Heterogeneous Nanocomposite Derived from Hematite and Rare-Earth Minerals*, **ACS Applied Materials & Interfaces, 8**, 2016, 20748−20755.

[8] D. Schubert, R. Dargusch, J. Raitano and S. W. Chan, *Cerium and yttrium oxide nanoparticles are neuroprotective*, **Biochemical and Biophysical Research Communications, 86**, 2006, 342.

[9] T. J. Brunner, P. Wick, P. Manser, P. Spohn, R. N. Grass and L. K. Limbach, *In Vitro Cytotoxicity of Oxide Nanoparticles: Comparison to Asbestos, Silica, and the Effect of Particle Solubility*, **Environmental Science and Technology, 40**, 2006, 4374-4381.

[10] D. S. Aydin, Z. Bayindir, M. Hoseini and M. O. Pekguleryuz, *The high temperature oxidation and ignition behavior of Mg–Nd alloys part I: The oxidation of dilute alloys*, **Journal of Alloys and Compounds, 569**, 2013, 35–44.

[11] J. Hongyun, N. Wang, L. Xu and S. Hou, *Synthesis and Conductivity of Cerium Oxide Nano Particles*, **Materials Letters, 64,** 2010, 1254–1256.

[12] S. Dhara, *Formation, Dynamics, and Characterization of Nanostructures by Ion Beam Irradiation*, **Critical Reviews in Solid State and Materials Sciences, 32**, 2007, 1-50.

[13] X. Xiang, X. T Zu, S. Zhuand and L. M. Wang, *Optical properties of metallic nanoparticles in Ni-ion-implanted α-Al_2O_3 single crystals*, **Applied Physics Letters, 84**, 2004, 52.

[14] P. Thakur, R. Kumar, J. C Cezar, N. brooks, A. Sharma, S. K.Arora, S. Gautum, A. Kumar, K. H.Chae and I. V. Shvets, *Evolution of magnetic nanophases of Ni embedded in Al_2O_3 (001) matrix by X-ray magnetic circular dichroism*, **Applied Physics Letters, 501**, 2011, 404-408.

[15] P. Kumar, P. Kumar, A. Kumar, R. C. Meena, R. Tomar, F. Chand and K. Asokan, *Structural, morphological, electrical and dielectric properties of Mn doped CeO_2*, **Journal of Alloys and Compounds, 672**, 2016, 543–548.

[16] L. R. Shah, A. Bakhtyar, Z. Hao, W. G. Wang, Y. Q. Song, H. W. Zhang, S. I. Shah and J. Q. Xiao, *Detailed study on the role of oxygen vacancies in structural, magnetic and transport behavior of magnetic insulator: Co–CeO_2*, **Journal of Physics: Condensed Matter, 21**, 2009, 486004.

[17] J. M. D. Coey, M. Venkatesan and C. B. Fitzgerald, *Donor impurity band exchange in dilute ferromagnetic oxides*, **Nature Materials, 4**, 2005, 173-179.

Received: June 27, 2017
Accepted: September 4, 2017